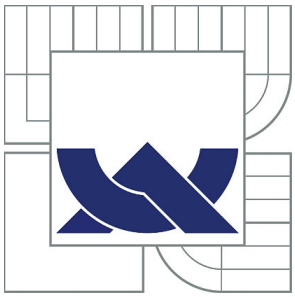

VYSOKÉ UČENÍ TECHNICKÉ V BRNĚ

BRNO UNIVERSITY OF TECHNOLOGY

FAKULTA STROJNÍHO INŽENÝRSTVÍ

ÚSTAV MECHANIKY TĚLES, MECHATRONIKY A BIOMECHANIKY

FACULTY OF MECHANICAL ENGINEERING

INSTITUTE OF SOLID MECHANICS, MECHATRONICS AND BIOMECHANICS

VYUŽITÍ MEMS TECHNOLOGIÍ V OBLASTI TERMOELEKTRICKÝCH GENERÁTORŮ

APPLICATION OF MEMS TECHNOLOGY IN THE FIELD OF THERMOELECTRIC GENERATORS

BAKALÁŘSKÁ PRÁCE

BACHELOR'S THESIS

AUTOR PRÁCE — LUDĚK JANÁK

AUTHOR

VEDOUCÍ PRÁCE — Ing. ZDENĚK ANČÍK

SUPERVISOR

BRNO 2012

Vysoké učení technické v Brně, Fakulta strojního inženýrství

Ústav mechaniky těles, mechatroniky a biomechaniky
Akademický rok: 2011/2012

ZADÁNÍ BAKALÁŘSKÉ PRÁCE

student(ka): Luděk Janák

který/která studuje v **bakalářském studijním programu**

obor: **Mechatronika (3906R001)**

Ředitel ústavu Vám v souladu se zákonem č.111/1998 o vysokých školách a se Studijním a zkušebním řádem VUT v Brně určuje následující téma bakalářské práce:

Využití MEMS technologií v oblasti termoelektrických generátorů

v anglickém jazyce:

Application of MEMS technology in the field of thermoelectric generators

Stručná charakteristika problematiky úkolu:

Rozvoj a budoucnost dnešní společnosti jsou kriticky závislé na schopnosti využití čistých, obnovitelných a nových zdrojů energie. Současným trendem a nezávislým oborem v této oblasti je Energy Harvesting, jehož cílem je využití energetických zdrojů volně dostupných v okolí. Jednou z nejvíce progresivních technologií v této oblasti jsou TermoElektrické Generátory (TEG), které s vývojem nových termoelektrických materiálů a výrobních technologií nabývají stále většího významu.

Cíle bakalářské práce:

1. Rešeršní studie současných trendů a využití MEMS technologií v TEG.
2. Modelování a optimalizace parametrů TEG.
3. Experimentální měření na reálné TEG jednotce.
4. Zhodnocení možností využití TEG v oblasti letecké techniky.

Seznam odborné literatury:

[1] Goldsmid, H.J.: Introduction to thermoelectricity, Springer, 2010
[2] Rowe, D.M.: Thermoelectrics handbook: macro to nano, Taylor & Francis Group, 2006
[3] Kozák, J.: Termoelektrický generátor, Bakalářská práce, FSI VUT Brno, 2011
[4] Dokumentace výrobců MEMS TEG

Vedoucí bakalářské práce: Ing. Zdeněk Ančík

Termín odevzdání bakalářské práce je stanoven časovým plánem akademického roku 2011/2012.

V Brně, dne 18.10.2011

L.S.

_____	_____
prof. Ing. Jindřich Petruška, CSc.	prof. RNDr. Miroslav Doupovec, CSc., dr. h. c.
Ředitel ústavu	Děkan fakulty

Abstrakt:

Práce je zaměřena na moderní oblast využití MEMS technologií v oblasti termoelektrických generátorů. Úvodem jsou diskutovány základní principy konstrukce a výroby MEMS TEG modulů. Praktická část práce sestává z ověření parametrů komerčního MEMS TEG modulu měřením a jeho simulace. Simulace je provedena pomocí MATLAB/Simulink i analytických metod. V závěru práce je na základě získaných poznatků provedeno zhodnocení využití metod „thermal energy harvesting" v oblasti letecké techniky.

Klíčová slova: MEMS, TEG, termoelektrický generátor, seebeckův jev, termoelektřina, energy harvesting, mikrosystémy.

Abstract:

This thesis is focused on the modern field of application of MEMS technology in the field of thermoelectric generators. The introductory part deals with fundamental principles of MEMS TEG construction and manufacturing. The practical part of this thesis consists of verification of commercial MEMS TEG parameters and its simulation. Simulation is carried out using MATLAB/Simulink as well as analytical methods. The conclusion deals with evaluation of use of thermal energy harvesting methods in aircraft-specific field.

Key words: MEMS, TEG, thermoelectric genarator, Seebeck Effect, thermoelectricity, energy harvesting, microsystems.

Bibliografická citace:

JANÁK, L. *Využití MEMS technologií v oblasti termoelektrických generátorů*. Brno: Vysoké učení technické v Brně, Fakulta strojního inženýrství, 2012. 46 s. Vedoucí bakalářské práce Ing. Zdeněk Ančík

Declaration on word of honour

I statutory declare, that I wrote this thesis: *Application of MEMS technology in the field of thermoelectric generators* by myself and under supervision of my instructor.

Brno 25.5.2012

_____

Luděk Janák

Acknowledgments

I would like to express my sincere gratitude to Ing. Zdeněk Ančík for enthusiastic guidance and knowledge support of this work.

I am also grateful for the interesting topic set by the mechatronical department of UNIS a. s. company headed by RNDr. Vladimír Opluštil.

My special thanks for the help with simulations and measurement belongs to Jakub Štetina and Bc. Jan Kozák.

Contents

Contents 8
1 Introduction 9
2 Fundamentals of MEMS technology 10
2.1 Definitions 10
2.2 Common features of MEMS 10
2.3 Applications of the MEMS 11
3 Fundamentals of thermoelectricity 12
3.1 Seebeck effect 12
3.2 Peltier effect 14
3.3 Other thermoelectric effects 15
3.4 Thermoelectric materials 15
4 Micro Thermoelectric Generators 17
4.1 MEMS TEG Design 17
4.2 Methods for Production of Thermoelectric Thin-Films 18
4.3 Outer Parameters 21
4.4 Trade Review 22
5 Measurement of MEMS TEG Performances 25
5.1 Test Stand Description 25
5.2 Open Circuit Voltage 26
5.3 Operation with Matched Load 27
5.4 Internal Resistance 28
6 Modeling of MEMS TEG 30
6.1 Simplified Model 30
6.2 Analytical Model of MEMS TEG with Contact Resistances 31
6.3 Equivalent Circuit 34
7 Comparison of Results of Used Methods 37
8 TEGs in Aircraft-specific Applications 38
8.1 Existing Solutions 38
8.2 Thermal Energy Harvesting Possibilities 38
Conclusion 40
References 41
List of Symbols 44
Appendix 46

1 Introduction

"There's Plenty of Room at the Bottom" (Richard Phillips Feynman) [1]

When Richard P. Feynman gave in the 1959 the famous lecture named as cited above, nobody knew how correct his considerations were. His lecture was about the forthcoming era of miniaturization, microsystems and nanosystems. Based on this lecture Feynman is often called the "Father of Nanotechnology".

Many years have passed. Nowadays the considerations from his talk which was focused mainly as a theoretical look-out are turned into practice as the MicroElectroMechanical Systems (MEMS) and the NanoElectroMechanical Systems (NEMS).

The advantages of miniaturization are not only low demands on space. It means, that there is not just a plenty of room at the bottom, but also many new aspects of known physical phenomena in the microsystems. With an increasing level of miniaturization significant changes occur in the phenomena of heat transfer, hydromechanics, lubrication, electrochemical and atomic processes.

This bachelor's thesis is focused on the MEMS technology in the field of ThermoElectric Generators (TEGs) and their use in aerospace applications.

Application of TEGs as the energy harvesting systems in aerospace applications is quite a new theme which has not yet been discussed in many scientific journals and only a few functional samples were made. The possible application of MEMS TEG in aircraft-specific field is their use for powering the autonomous sensor nodes for structural health monitoring and powering the wireless sensors in general. In comparison with other energy harvesting technologies the main advantages for the use of TEGs in aviation are no movable parts allowing low demands on maintenance and mainly the presence of ideal conditions for thermal energy harvesting – natural heat gradient on the surface of aircraft. Other sources of heat involving engine, engine exhaust and heat from passengers could be also taken into an account.

The task of this thesis is to make the review of available MEMS TEG technologies for energy harvesting, compile the manufacturer's data and make the computational model based on this search. The computational model will be also verified by the measurement on the real MEMS TEG module. The last point of this work is the evaluation of examined TEG modules for use in the field of aircraft-specific applications. All of these tasks are based on submission set by mechatronical department of UNIS a. s. company.

This thesis begins in Chapter 2 by short introduction into the scaling of miniature devices and necessary definitions connected with this field. Chapter 3 deals with general principles and basic considerations such as thermoelectric effects and basic relations in thermoelectric theory. Chapter 4 is concerned with suitable MEMS TEGs and their parameters and gives a brief overview of the market. Chapter 5 shows the measurement procedure, measuring stand and interpretation of measured results. Chapter 6 describes the model building based on further understanding of thermal and electrical processes in TEG and shows more possible ways to describe TEG. Chapter 7 compares the data gained from various models, measurement and manufacturers datasheets. The last Chapter 8 provides major conclusions about possibilities for use of MEMS TEGs in aircraft-specific applications and outlines the pathways for the future development.

2 Fundamentals of MEMS technology

2.1 Definitions

Microelectromechanical systems (MEMS) refer to devices that have a characteristic length of less than 1 mm but more than 1 μm, that combine electrical and mechanical components and that are fabricated using integrated circuit batch-processing technologies. [2]

Nanoelectromechanical systems (NEMS) are made of electromechanical devices that have critical dimensions from hundreds down to a few nanometers. By exploring nanoscale effects, NEMS present interesting and unique characteristics, which deviate greatly from their predecessor microelectromechanical systems (MEMS). [3]

The graphical interpretation of definitions mentioned above is given in the Fig. 1. As can be seen in the Fig. 1, the characteristic length of MEMS is comparable with the thickness of a human hair. The smallest man-made devices have the dimensions of about only ten times greater than a hydrogen atom which causes the unique characteristics of NEMS devices such as fundamental frequencies in gigahertz (microwave) range, force sensitivity at the attonewton level, power consumption in tens of attowatts and extremely high integration levels up to 10^{12} elements per square centimeter [3]. In the further reading we will be focused only on the field of MEMS.

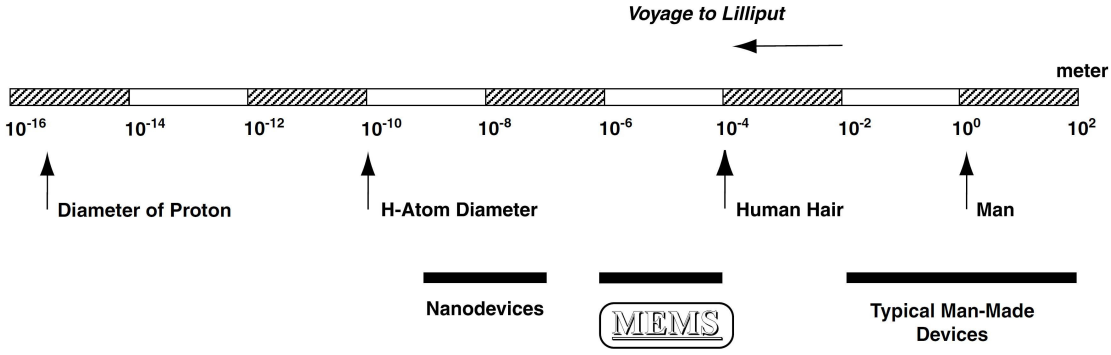

Fig. 1 – Scaling of miniature devices [2]

2.2 Common features of MEMS

The definition of MEMS gives an austere understanding about the MEMS sizing but neglects some important features of MEMS. According to [4] the common features of MEMS are as follows:

- MEMS involve always the electronic and non-electronic parts (mechanical parts which could be movable or non-movable) and perform functions such as signal acquisition (sensing), signal processing, actuation, display and control. The important role for MEMS is also use in the field of chemical and biochemical reactions and assays.
- MEMS are systems in the true sense – which means, that typical system features such as stability, step response, signal-to-noise ratio, reliability but also calibration and packaging have to be considered during the design process.

- The important step during the MEMS design is disuse of classical “macro” approach to the systems functions and design. MEMS are not simply size-reduced “macro” systems. The most successful MEMS are based on new phenomena which occur at the “micro” level. As an examples could be given the ink-jet print heads or thin film magnetic disk heads.
- Some MEMS could consist of large arrays of microfabricated elements (e.g. periodical structures of P-N junctions) which could finally causes that the size of MEMS is greater than 1 mm.

2.3 Applications of the MEMS

The MEMS technology could be used and useful in all fields of engineering and in some fields of medicine, chemistry and biosciences. The current implementation of the MEMS technology involves sensors for pressure, temperature, mass flow, velocity, sound and chemical composition and actuators for linear and angular motions. MEMS could be, of course, used as components for design and build of higher complex systems such as robots, micro heat engines and micro heat pumps. Applications of MEMS in biosciences as biosensors and micro reactors may play an important role. [2]

MEMS are currently used as parts of complex systems in accelerometers for automobile airbags, keyless entry systems, dense arrays of micromirrors for high-definition optical displays, scanning electron microscope tips to image single atoms, micro heat exchangers for cooling of electronic circuits, blood analyzers and pressure sensors for catheter tips. Micropumps are used for ink-jet printing, environmental testing and electronic cooling. Potential medical applications involve systems for targeted drug delivery and manufacturing of nanoliters of chemicals. The most relevant application for the purpose of this thesis is in the field of energy harvesting. The MEMS energy scavengers could be based on the thermoelectric, piezoelectric, electromagnetic or electrochemical phenomena. [2]

The application fields for MEMS could be divided into 7 main areas as shown below. This division is based on the MEMS worldwide market review from 2009 mentioned in [4]:

- temperature sensors (including thermoelectric generators)
- magnetic field sensors (micro hall probes)
- microfluidics (ink-jet printers, mass-flow sensors, biolab chips)
- pressure sensors (automotive, medical, industrial)
- accelerometers
- optical MEMS (optical switches, displays)
- other MEMS and actuators (micromotors, microturbines).

This thesis is focused only to the field of MEMS technologies applied on TEGs. A comprehensive review of other MEMS is given in [2, 4-5].

3 Fundamentals of thermoelectricity

The history of theory of thermoelectric generation goes back to 1821. In this year T.J. Seebeck found that the heated junction of two different electrical conductors could produce an electromotive force. Seebeck used two different metals which caused the insignificant amount of produced electrical energy.

Thirteen years after Seebeck made his discovery, a French watchmaker J. Peltier found the reverse effect. He realized that passage of electrical current through the junction of two different conductors could produce a small heating or cooling effect dependant on the direction of the passing current.

Very interesting historical notice about Seebeck and Peltier is that they didn't know that their discoveries are related to the each other. The theory of thermoelectricity has been unified in 1855 by a well-known theoretician W. Thomson (Lord Kelvin) who applied the thermodynamic theory to the problem and find out the third thermoelectric effect which is applied in every homogenous conductor – the Thomson effect. [6]

3.1 Seebeck effect

The Seebeck effect is based on the diffusion of electrons through the interface between two different materials – conductors or semiconductors. This diffusion is achieved by applying a heating at the junction of the materials. Heating causes the net changes in the materials and allows electrons to move from material where they have lower energy into material where the energy of electrons is higher. Because the electrical current is exactly a flow of electrons, this effect of passing electrons from one material to another makes an electromotive force (voltage) on the terminals of thermoelectric module. Generated voltage is linearly dependant on the temperature difference between hot and cold sides of thermoelectric module. The graphical interpretation is given in the Fig. 2. [6-8]

Voltage value is given as:

$$U = \alpha_{AB}.(T_H - T_C) \tag{3.1}$$

where:

- α_{AB} differential Seebeck coefficient
- U voltage
- T_H temperature of the hot side
- T_C temperature of the cold side.

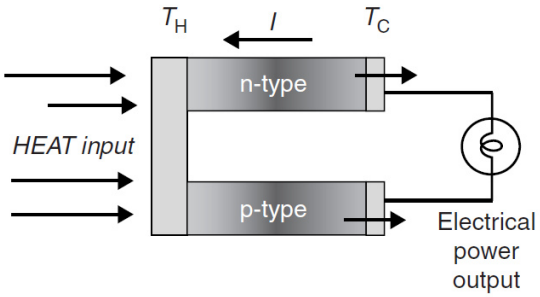

Fig. 2 – Seebeck effect [7]

Although it seems that Seebeck effect could be an interfacial phenomenon that is nondependent on bulk properties of the material the opposite is true. Voltage measured on the terminals of thermoelectric module is linearly dependent on the Seebeck coefficient which is a material property:

$$\alpha_{AB} = \frac{U}{\Delta T} \tag{3.2}$$

where:

- α_{AB} differential Seebeck coefficient
- U voltage
- ΔT temperature difference ($T_H - T_C$).

Thus a value of the differential Seebeck coefficient is a material characteristic of the junction we define it using Seebeck coefficient of both two materials:

$$\alpha_{AB} = \alpha_A - \alpha_B \tag{3.3}$$

where:

- α_{AB} differential Seebeck coefficient
- α_A Seebeck coefficient of material A
- α_B Seebeck coefficient of material B.

Notable thing about the thermoelectric energy conversion is their efficiency. We define the efficiency of thermoelectric energy conversion as the division of energy supplied to the load and heath flow through the hot side of thermoelectric module [6-8]:

$$\eta = \frac{E_e}{Q_H} \tag{3.4}$$

where:

- η efficiency
- E_e electrical energy supplied to the load
- Q_H heath flow through the hot side.

Thermocouple is, in fact, a type of heat engine operating between two temperatures of cold and hot side – T_H and T_C. Thus a theoretical efficiency of the thermoelectric energy conversion is limited by the Carnot cycle rules [7]:

$$\eta_{CARNOT} = \frac{\Delta T}{T_H} \tag{3.5}$$

where:

- η_{CARNOT} theoretical (Carnot cycle) efficiency
- ΔT temperature difference
- T_H temperature of the hot side.

The real efficiency of thermoelectric conversion is always lower than theoretical. Common value of efficiency is about 14 % of Carnot efficiency using bulk

semiconductors around room temperature. In the further reading will be shown that efficiency could be expressed using material properties values. [8]

3.2 Peltier effect

The Peltier effect is inverse phenomena to the Seebeck effect. The physical meaning of the Peltier effect is also diffusion of electrons but in the opposite direction than in the case of Seebeck effect. The electromotive force is now the source of electrons kinetic energy and heating at the junction is a product of electrons movement. Applications of this effect include cooling in various environments. The graphical interpretation of the Peltier effect is given in the Fig. 3. [6-8]

We define the Peltier coefficient witch is giving into account pumped head and electrical current supplied to the thermoelectric module:

$$\pi_{AB} = \frac{q}{I} \tag{3.6}$$

where:

- π_{AB} Peltier coefficient
- q heat pumped through the thermoelectric module
- I electrical current.

Because the Peltier coefficient is much more difficult to measure than the Seebeck coefficient we use the conversion equation to reach them from known value of Seebeck coefficient:

$$\pi_{AB} = \alpha_{AB} T \tag{3.7}$$

where:

- π_{AB} Peltier coefficient
- α_{AB} differential Seebeck coefficient
- T temperature.

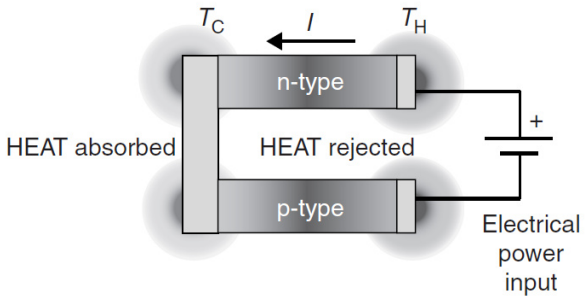

Fig. 3 – Peltier effect [7]

3.3 Other thermoelectric effects

Theory of thermoelectricity deals with three main thermoelectric effects – Seebeck, Peltier and Thomson. The Thomson effect is being applied in every homogenous conductor which is given along the temperature gradient and is passed by an electrical current. The Thomson effect could be neglected in the wide range of calculations instead of very precise models. [6, 7]

Applying a magnetic field into problem of thermoelectricity could be find another 2 effects connecting with interaction of thermal, electric and magnetic field. These effects are called after Nernst and Ettinghausen. The Nernst effect is analogy of Seebeck in magnetic field. Its application is sometimes in the detection of thermal radiation. The Ettinghausen effect – analogy of Peltier – could be potentially applied in refrigeration at low temperatures. [6]

3.4 Thermoelectric materials

Although at the beginning of thermoelectric era Seebeck and Peltier used metal conductors to demonstrate thermoelectric effects these materials seems disadvantageous nowadays. Thermoelectric effects in metals are strongly suppressed by the Joule heating. The best materials for thermoelectric energy conversion are heavily doped semiconductors. [9]

Suitability of material for the thermoelectric energy conversion could be evaluated using the figure of merit:

$$ZT = \frac{\alpha^2}{\lambda\rho} T \tag{3.8}$$

where:

- ZT figure of merit
- α Seebeck coefficient
- λ thermal conductivity
- ρ electrical resistivity
- T temperature.

Higher figure of merit indicates the higher suitability of use the material for thermoelectric energy conversion. As could be easily proven from ZT expression, ideal thermoelectric material should have high Seebeck coefficient, low thermal conductivity and electrical resistance. Increase of the figure of merit is the task for MEMS TEGs. [6-8]

Materials with $ZT > 0.5$ are called thermoelectric materials. The thermoelectric materials are conveniently divided into three groups with respect to the operating temperatures. This distribution is mentioned in the Fig. 4. Alloys based on bismuth in combinations with antimony, tellurium and selenium are classified as low-temperature thermoelectric materials for temperatures of up to 450 K. Middle temperature range 450 – 850 K is a domain for lead telluride materials. For the highest temperature range up to 1300 K are used germanium alloys. [7]

As mentioned in 3.1 the efficiency of thermoelectric generator could be expressed by bulk properties of used material. Properties are represented by the figure of merit ZT:

$$\eta = \frac{\Delta T}{T_H} \cdot \frac{\sqrt{1+ZT}-1}{\sqrt{1+ZT}+\frac{T_C}{T_H}} \tag{3.9}$$

where:

- η efficiency
- ΔT temperature difference
- T_H temperature of the hot side
- T_C temperature of the cold side
- ZT figure of merit.

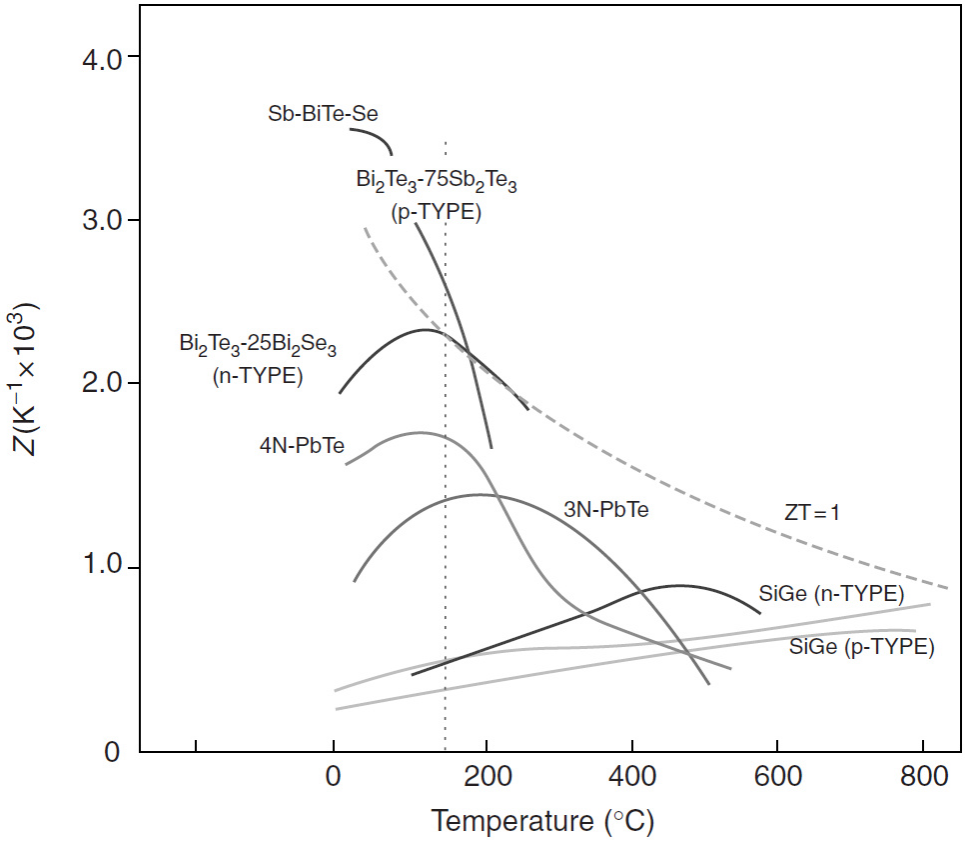

Fig. 4 – Recent thermoelectric materials properties [7]

4 Micro Thermoelectric Generators

Implementation of the MEMS technology in TEGs is based on miniaturization of thermocouples made of semiconductor thermoelectric materials using special thin-film manufacturing technologies. This approach affects the minimization of thermal conductivity, prospective maximization of electrical conductivity, increase of number of thermocouples and last but not least the high power density.

Current technology development in the miniaturization of thermoelectric generators is spread over three main pathways [7]:

- *Enhancement of the thermoelectric figure of merit (FOM) ZT. This performance can be significantly enhanced to ZT >> 1 by employing nanostructred materials such as quantum wells, superlattices, nanowires, and nanograins.*
- *Use of miniaturized designs by adopting techniques typical for MEMS devices.*
- *The transfer of manufacturing techniques originating from CMOS microelectronics to mass production.*

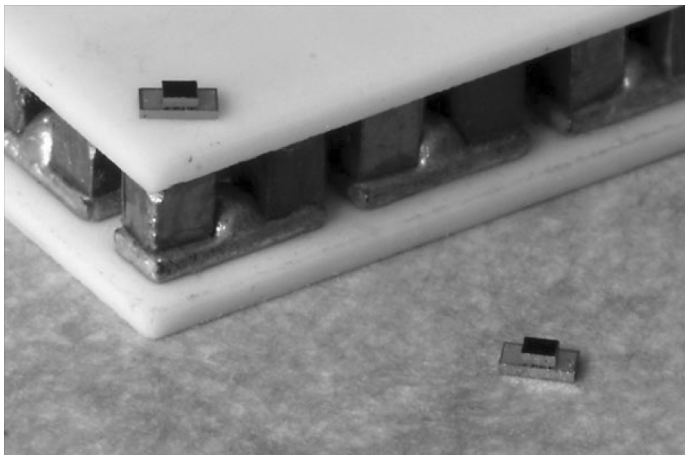

Fig. 5 – Comparison of classical and MEMS TEG [7]

4.1 MEMS TEG Design

Every MEMS TEG is made of a large number of thermocouples connected electrically in series and thermally in parallel. There are two main approaches to the MEMS TEG design setup – lateral/lateral and vertical/vertical. In the case of Lateral/lateral type is the heat flow or temperature difference applied in the same direction as thermocouples laterally to the substrate. In the case of vertical/vertical type are the heat flow and thermocouples applied vertically to the substrate. It's also possible to combine lateral and vertical approach which is called vertical/lateral type. Commercially available TEGs are being produced using vertical/vertical design only. [7, 9-11]

The common MEMS thermoelectric generator has than a similar geometry as standard thermoelectric generator. However their geometrical difference is a difference in size. Standard thermoelectric generator size could be about 34 x 30 mm with 4 mm thickness [12]. On the other hand the size of typical MEMS TEG is about 3.3 x 3.1 mm with 0.6 mm thickness [13]. Even more significant differences are in the length of thermocouples. Thermocouples integrated in a classical TEG have a length about 3 mm when a thin-film layer of miniaturized P-N thermocouples has 70 μm.

Design of vertical/vertical MEMS thermoelectric generators has the well established pattern which can be found in a large number of implementations (Fig. 6). Common MEMS TEG could be decomposed into the following parts [7]:

- **Hot side** – part of TEG which is attached to the spot with higher temperature, usually to the heat source.
- **Cold side** – part of TEG which is attached to the spot with lower temperature, usually to the heat sink.
- **Substrate (wafer)** – base plate to which are deposited thermocouples. Substrate is usually made of Si. Many technical realizations are based on two wafer principles – hot and cold sides of the TEG module are produced at first separately, one with thin-film of P semiconductors and other with N, then are connected together – like two slices of a wafer.
- **Thermocouples** – thin-film based, deposited by microfabrication technologies. For the P-N thermocouples of commercially available modules are used low-temperature thermoelectric materials Bi_2Te_3 and $(Bi, Sb)_2Te_3$. Thermocouple footprint is very small. Side lengths are usually tenths to hundreds of micrometers
- **Junctions** – conductive connections of P-N thermocouples. Junctions could be realized by heavily doped layers of substrate in the connection points or by soldering of thermocouples using metallic solder.
- **Insulation** – insulates thermocouples from both thermal and electrical point of view.
- **Wire bondable pads** – spots for interconnection with superior system via PCB or wires.
- **Wires** – soldered to the wire bondable pads for the easy connection to the superior system. On the commercially available modules usually on request.

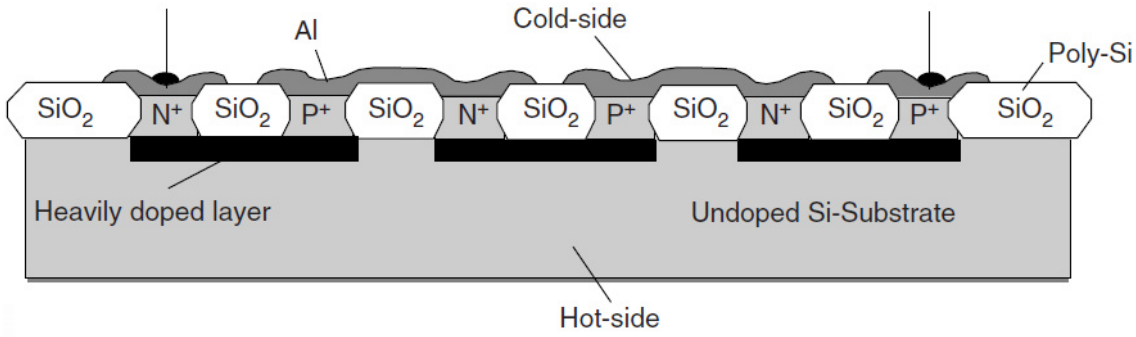

Fig. 6 – Vertical/vertical MEMS TEG design setup [7]

4.2 Methods for Production of Thermoelectric Thin-Films

Although the geometry of MEMS and standard thermoelectric generators is exactly the same but smaller, the methods of their production are quiet different.

Classical thermoelectric generators are usually made of bulk materials using conventional manufacturing methods. The mostly used methods are growth from the melt and sintering. Acquired bulk material is than sliced out of the block of bulk material and placed in the appropriated direction for reaching the maximum *ZT* to the conducting substrate. This technological step is assigned into the manufacturing process

because the (poly)crystalline materials *ZT* is strongly dependant on the direction which the heat flow passes through. This dependence is given by different mobility of electrons in different ways. For the commonly used low-temperature thermoelectric materials Bi_2Te_3 and $(Bi, Sb)_2Te_3$ the high $ZT \sim 1$ direction is achieved when the heat flow is applied perpendicularly to the crystalline C-axis. When the heat flow is passing parallel to the C-axis, the *ZT* is much lower – around $ZT \sim 0.5$. The whole phenomenon is shown in the Fig. 6. [6-7]

From the considerations above could be clearly proven that the key request for the microfabrication techniques is possibility for orientation of crystals in the high *ZT* direction. Unfortunately the manipulation at the microscale is not as simple as at the macroscale. Generally is very difficult to achieve the high *ZT* direction when using microfabrication techniques. Thus the wide range of manufacturing techniques which allows producing MEMS TEGs with chaotically located polycrystals exists. Materials produced in this way are often called "materials with average *ZT*". The maximum figure of merit *ZT* could achieve about 0.75 in this case.

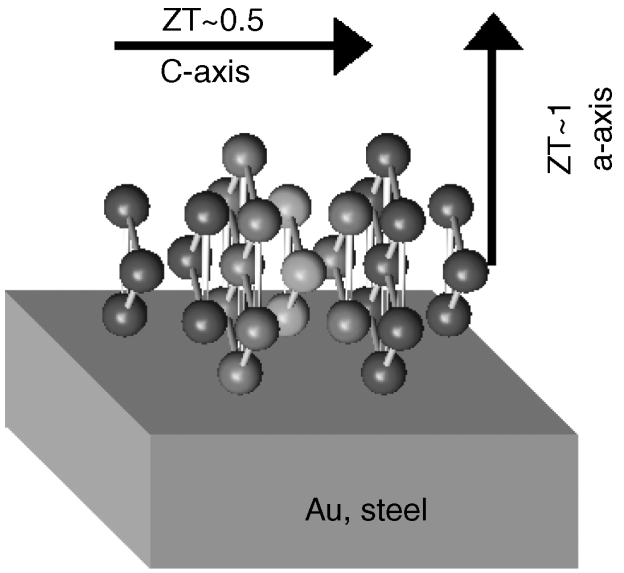

Fig. 7 – Crystalline orientation of deposited Bi_2Te_3 [7]

Currently used manufacturing technologies for deposition of thin-film thermocouples in the field of MEMS thermoelectric generators are usually taken over CMOS technology, microelectronics technology and thin-film optical technology. Commonly used manufacturing technologies are listed below [9]:

- **Sputtering** – established PVD (Physical Vapour Deposition) method for producing materials with the average *ZT*. Inert sputtering gas is ionized and accelerated by electric field previously. Molecules of thermoelectric material are knocked out from the sputtering target after interaction with accelerated inert gas. Thermoelectric material is sputtered onto the substrate consequently (Fig. 7). Whole process is performed in low-pressure environment. This method is used in a mass production by Micropelt GmbH. Results of this method are shown in the Fig. 8. [4, 14]

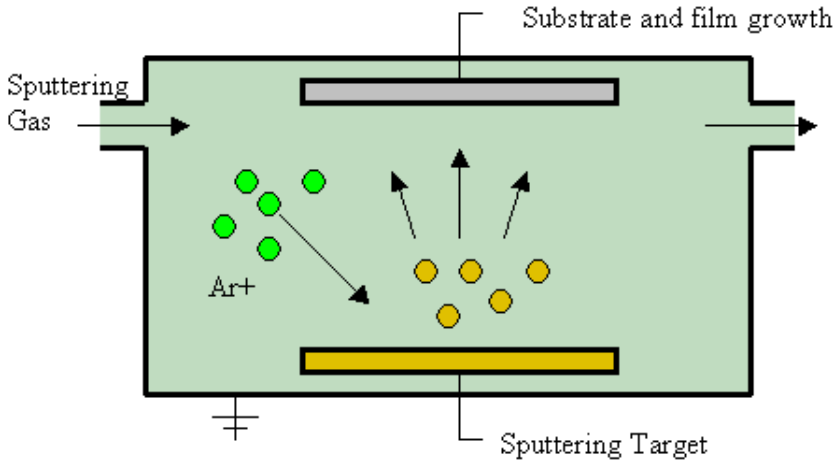

Fig. 8 – Sputtering [17]

- **CVD (Chemical Vapour Deposition)** – chemical process adapted from semiconductor industry. The wafer (substrate) is exposed to the one or more precursors which contains source materials in the heated furnace. Required thin-film on the surface of substrate is grown after the chemical reaction of precursors. Precursors entering the furnace in the gas phase. Often used precursors in the field of thermoelectric materials are metalorganics and hydrides. Technology based on these precursors is called MOCVD (Metal-Organic Chemical Vapour Deposition). Whole process is performed in low-pressure environment. Method is used by Nextreme Thermal Solutions, Inc. Results of this method are shown in the Fig. 8. [4, 15, 16, 18]

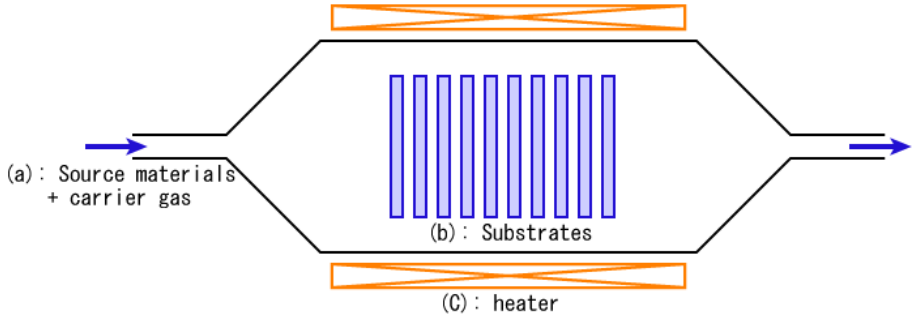

Fig. 9 – CVD [17]

- **Thinning of bulk material** – derived from classical Bi_2Te_3 production technology and adapted to reach a minimal P-N legs thickness. Achievable final thickness of thermocouple legs is about 200 μm which causes ΔT_{max} ~ 70 K and Q_{max} ~ 80 W.cm^{-2}. This method is not commonly used for the mass production. [7]
- **Electrodeposition** - the only thin-film manufacturing technology which could achieve the high *ZT* direction of polycrystals. Electrodepostition is based on the electrophoresis principles. Colloidal particles are deposited onto an electrode after their migration in liquid medium under the influence of electric field. Electrodeposition of Bi_2Te_3 is a quite difficult topic which is nowadays carried out in experimental laboratory conditions (e.g. JPL). No device has been fabricated to date using this technology. [7]

After the thin-film growth are usually applied the finalization processes. The thin film applied on wafer is finalized to the final shape using a pattern transfer. The desired pattern is firstly transferred from mask by the photo-process to the wafer surface. Then the chemical or physical process for subtracting the excess thin-film is applied. Often used method in the field of micro TEGs is wet etching. [4, 9]

Because the wafers with P and N thin-film legs are often produced separately (two wafer concept), the last processing step in the production of MEMS TEG is a connection of both – P and N - wafers. The connection could be made using soldering.

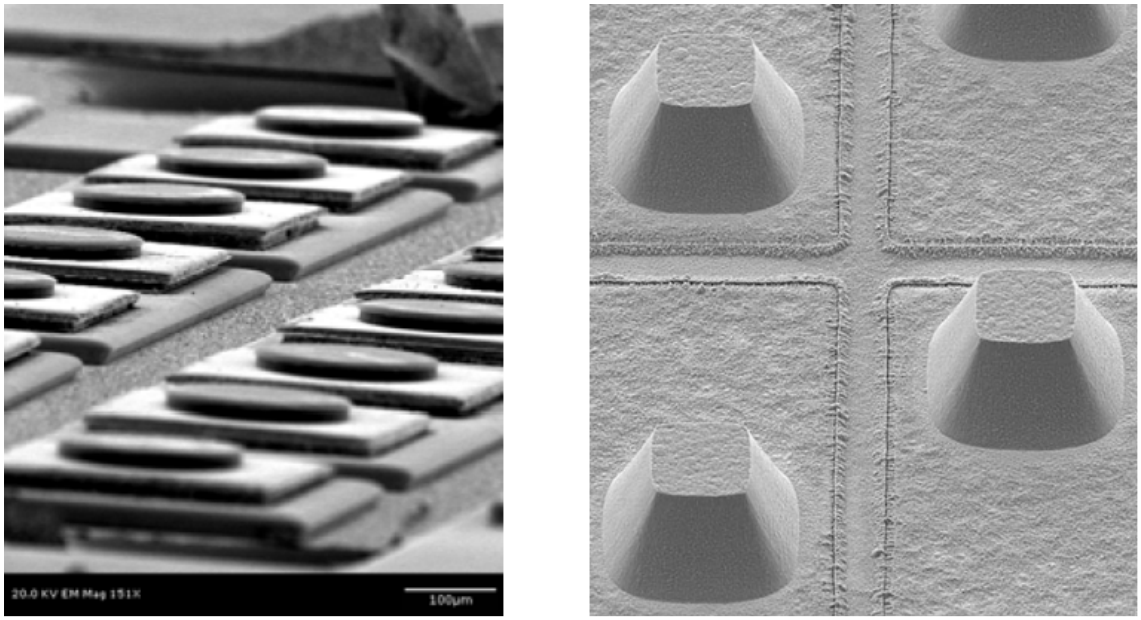

Fig. 10 – Thermocouple legs deposited using CVD (left) and sputtering (right), not in scale [14, 18]

4.3 Outer Parameters

Last paragraphs deal with an internal point of view on MEMS TEG. It's useful when thinking about microscale physical processes and for further understanding of MEMS TEG devices. When considering about the use of TEG as an electrical power source for supplying a complex system it's appropriate and concurrently enough to specify outer parameters of MEMS TEG. The most important parameters from the "system point of view" are:

- **Dimensions** – footprint and module thickness. This parameter is necessary due to design of mounting and space requirements.
- **Thermal resistance R_T** – is required the maximum possible. High thermal resistance provides a quality thermal separation of hot and cold side allowing the high temperature difference according to Fourier's law.
- **Internal electrical resistance R_i** – is required the minimum possible. R_i negatively affects V-A curves of TEG.
- **Net seebeck voltage** – represents the generated open circuit voltage per one Kelvin on the terminals of TEG.

- **Open circuit voltage U_{oc}** – is a property dependant on applied temperature difference. U_{oc} represents voltage on the terminals without load on desired temperature.
- **Maximum power** – is achieved when the load resistance is the same as internal resistance of TEG. This situation is called "maximum power point". In this setting are measured output voltage U_{out}, current I_{out} and power P_{out} applied to the load.
- **Power density P_{out}/A** – represents the electrical power applied to the load per square area of the TEG module.
- **Operating temperatures** – indicates the spans of temperatures applied to the hot and cold side (T_H and T_C), maximal temperature difference ΔT and exceptionally maximum mean temperature $T_{mean,max}$ in TEG cross section.

4.4 Trade Review

There are only a few existing commercial solutions in the field of MEMS TEGs and even fewer amount could be bought as a standalone solution. Concurrently some build-in solutions kept by worldwide commercial electronics manufacturers have been developed. Build-in MEMS TEGs for powering wristwatches developed by Seiko and Citizen might be taken as an example. It seems that wide commercial use of the MEMS thermoelectric generators is in its infancy. [7-9, 19]

Nevertheless there are some MEMS TEG manufacturers on the world market. Technologies held by these manufacturers were often developed by the principles of spin-off companies or technology transfer from universities and scientific institutions to the commercial sector.

Based on literature and internet search were found the following companies interested in the standalone MEMS TEG solutions:

- Micropelt GmbH [20]
- Nextreme Thermal Solutions, Inc. [21]
- Thermo Life® Energy Corp., Inc. [22]
- Hi-Z Technology, Inc. [23]
- Perpetua Power Source Technologies, Inc. [24]

Modules from the first two above-mentioned manufacturers – Nextreme and Micropelt – are currently easily achievable through worldwide electronics components retailers. Parameters of available modules from these manufacturers are compared in Tab. 1 and Tab. 2.

In Tab. 1 are given the temperature non-dependant data such as geometrical and thermal parameters. Tab. 2 deals with electrical parameters dependant on temperature. As a reference was selected 10 °C temperature difference. Data in these tables were extracted from the manufacturer's datasheets [13, 25-27]. Data which are not directly given in datasheets were deducted from graphs. Unavailable items are replaced by "-".

Tab. 1 – Commercially available MEMS TEGs properties

	eTEG HV14 (Nextreme)	**eTEG HV37 (Nextreme)**	**eTEG HV56 (Nextreme)**	**MPG-D651 (Micropelt)**	**MPG-D751 (Micropelt)**
***Footprint* [mm]**	1.8 x 1.5	3.39 x 2.05	3.31 x 3.12	3.375 x 2.5	4.248 x 3.364
***Square area* [mm^2]**	2.7	6.95	10,34	8.44	14.29
***Thickness* [mm]**	0.6	0.56	0.57	1.09	1.09
T_H [°C]	25-200	25-200	25-200	200	200
T_C [°C]	0-50	0-50	0-50	-	-
ΔT [°C]	15-200	15-200	10-200	-	-
$T_{mean,max}$ [°C]	150	150	150	-	-
***Number of thermocouples* [-]**	18	48	72	286	540
R_T [K/W]	46	21	13.1	22	12.5
R_i [Ω]	-	7.4	10.7	185	300
***Net Seebeck voltage* [mV/K]**	8	17.5	25	75	140

From Tab. 1 is evident that the thermal resistance of the smallest module eTEG HV14 is significantly higher than of larger ones. The number of thermocouples in TEGs produced by Micropelt is much greater which enables to achieve the high Seebeck net voltage but negatively affects the internal resistance of the module.

Tab. 2 – Commercially available MEMS TEGs properties on ΔT = 10 °C

	eTEG HV14 (Nextreme)	**eTEG HV37 (Nextreme)**	**eTEG HV56 (Nextreme)**	**MPG-D651 (Micropelt)**	**MPG-D751 (Micropelt)**
U_{oc} [V]	0.08	0.18	0.26	0.75	1.25
P_{out} [mW]	-	1	1.5	0.8	1.5
I_{out} [mA]	-	12	12	1.8	2
U_{out} [V]	-	0.09	0.13	0.45	0.75
I_{sc} [mA]	-	24	24	3.5	3.9
P_{out}/A [mW/ mm^2]	-	0.14	0.15	0.09	0.1

From Tab. 1 could be seen the voltage-current characters of the examined TEG modules. The Micropelt modules are constructed to maintenance higher voltages with lower current consumption. On the other hand the Nextreme modules could provide currents of tenths of milliamperes. Resulting power outputs of comparable TEGs of both companies are equal. Comparable TEG modules are eTEG HV37 vs. MPG-D651 and eTEG HV56 vs. MPG-D751.

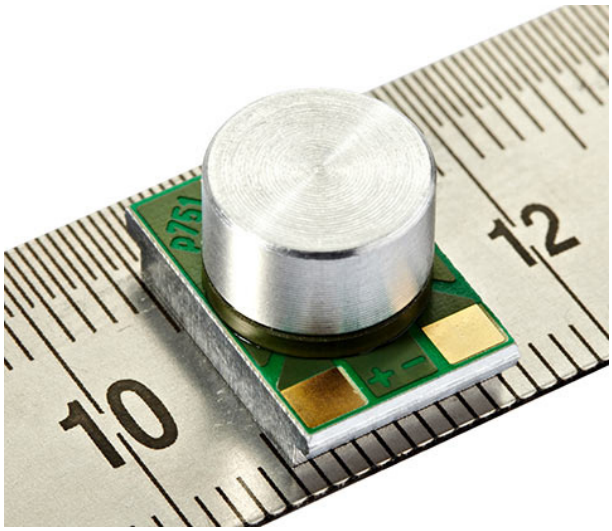

Fig. 11 – Micropelt MPG TEG mounted in package with 15x10 mm footprint [28]

For the purposes of models building and first verification measurement has been selected the eTEG HV56 from Nextreme Thermal Solutions, Inc. Module is shown in the Fig. 12. For the purposes of comfortable manipulation in the test stand has been selected the wired version. Datasheet of this TEG is in [App. 5].

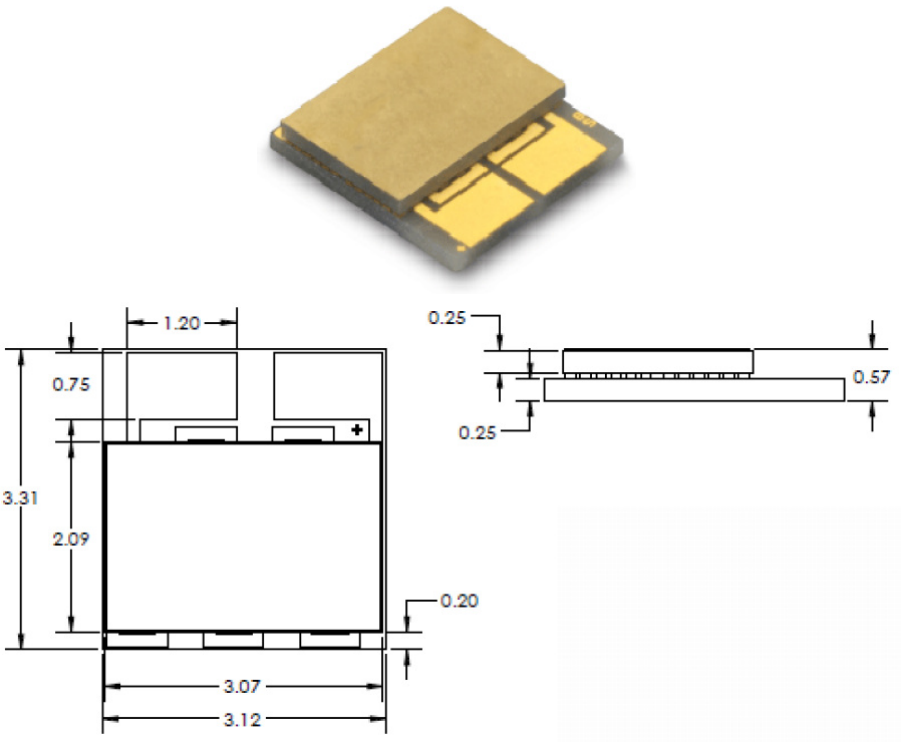

Fig. 12 – Nextreme Thermal Solutions eTEG HV56 [13]

5 Measurement of MEMS TEG Performances

For the purposes of measurement on the selected micro TEG module was used measurement stand briefly described in [29]. This device has been originally intended for determination of parameters of commonly available peltier modules with footprints up to 40 x 40 mm. The tested eTEG HV56 dimensions are many times smaller. The measuring stand has been adapted to accommodate this micro TEG.

5.1 Test Stand Description

The temperature difference is maintained by two peltier coolers. First peltier cooler is used as a heater placed at the bottom of test stand. Another one which operates in cooling mode is attached on the top to the heat sink which is then cooled by fan. Contact between the tested thermoelectric generator and peltier modules is ensured by aluminum plates in which are mounted temperature sensors. Test stand is insulated from surrounding environment by the cork container. The test stand is shown in the Fig. 13.

Modification of the test stand consists of newly drilled holes for MEMS TEG wires and insulation of unused contact surface among aluminum plates by paper layer. The contact thermal resistance minimization is reached using plastic fastening straps around the container and heat sink. Straps providing the necessary contact pressure between the surfaces.

Whole system is feedback controlled via MATLAB/Simulink. The interface with computer is realized by Humusoft MF624 card which allows to measure on high sampling frequencies.

Unfortunately the time-response of the measuring stand is very slow. Maintenance of temperature is based on hysteresis which causes the large ripple in hot and cold side temperatures. The ripple is also reflected in the temperatrure difference and output voltage on TEG. Slow time response causes the slow temperature ramp at the beginning of measurement. Error was eliminated by disuse of this ramp in evaluated data. Temperature difference (ΔT_{set}) ripple was eliminated by use of mean values for measured temperature (ΔT) and voltage. Typical raw data could be found in the Fig. 14.

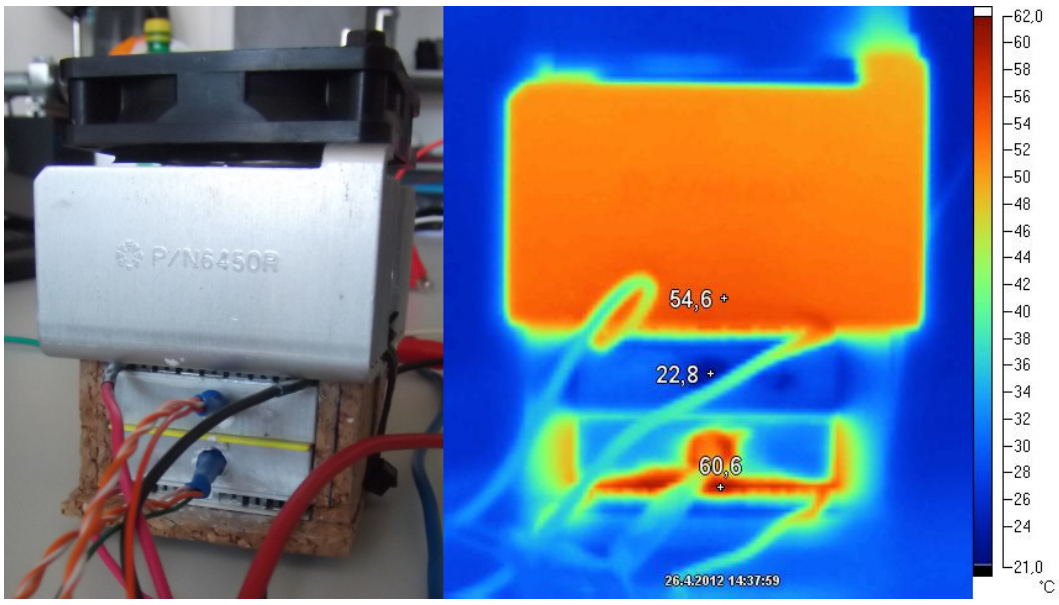

Fig. 13 – Test stand viewed in the visible and IR spectra during measurement process

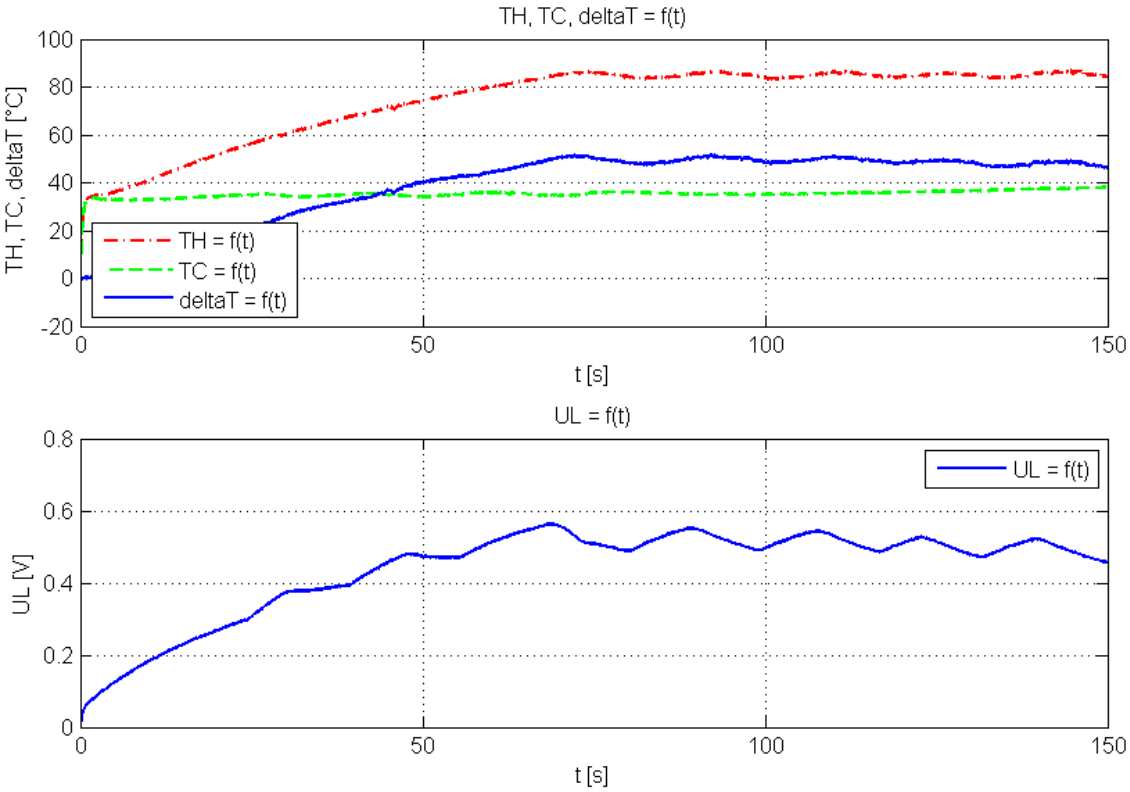

Fig. 14 – Raw data from measuring stand

The cold side temperature of $T_C = 35$ °C was maintained during whole measurement process. The hot side temperature was set with respect to the required temperature difference in each measurement.

5.2 Open Circuit Voltage

The open circuit voltage measurement was made simply by setting the temperatures of cold and hot sides in control software thus by the setting of required temperature difference. Measured data are listed in Tab. 3. Dependence of open circuit voltage U_{oc} on increasing temperature difference ΔT should be linear. The measured data are linearly fitted in the Fig. 15 to illustrate this relationship.

Tab. 3 – Open circuit voltage U_{oc} measurement

ΔT_{set} [°C]	ΔT [°C]	U_{oc} [V]
5	6.2	0.157
10	11.0	0.241
15	16.5	0.362
20	20.0	0.403
25	26.2	0.522
30	30.9	0.591
35	35.2	0.675
40	40.4	0.764
45	45.3	0.878
50	49.9	0.962

5.3 Operation with Matched Load

In the next step were measured the matched load parameters of TEG – voltage U_L, current I_L and power P_L. Because the internal resistance hasn't been still determined by measurement, the value from Tab. 2 was used and the nearby load resistance of 10 Ω was applied. Measured data are listed in Tab. 4. The voltage U_L is the only one directly measured electrical parameter. Another data are derived using Ohm's law. The voltage is again linearly fitted and shown in the Fig. 15. From this measurement was also obtained the power output dependence on temperature difference. This dependence is quadratic approximated by the polynomial fit of second order.

Tab. 4 – Operation nearby matched load

ΔT_{set} [°C]	ΔT [°C]	R_L [Ω]	U_L [V]	I_L [mA]	P_L [mW]
5	7.1	10	0.104	10.4	1.082
10	11.0		0.145	14.5	2.103
15	15.7		0.167	16.7	2.789
20	21.3		0.239	23.9	5.712
25	26.0		0.287	28.7	8.237
30	30.7		0.334	33.4	11.156
35	35.3		0.379	37.9	14.364
40	40.1		0.426	42.6	18.148
45	44.8		0.471	47.1	22.184
50	49.6		0.518	51.8	26.832

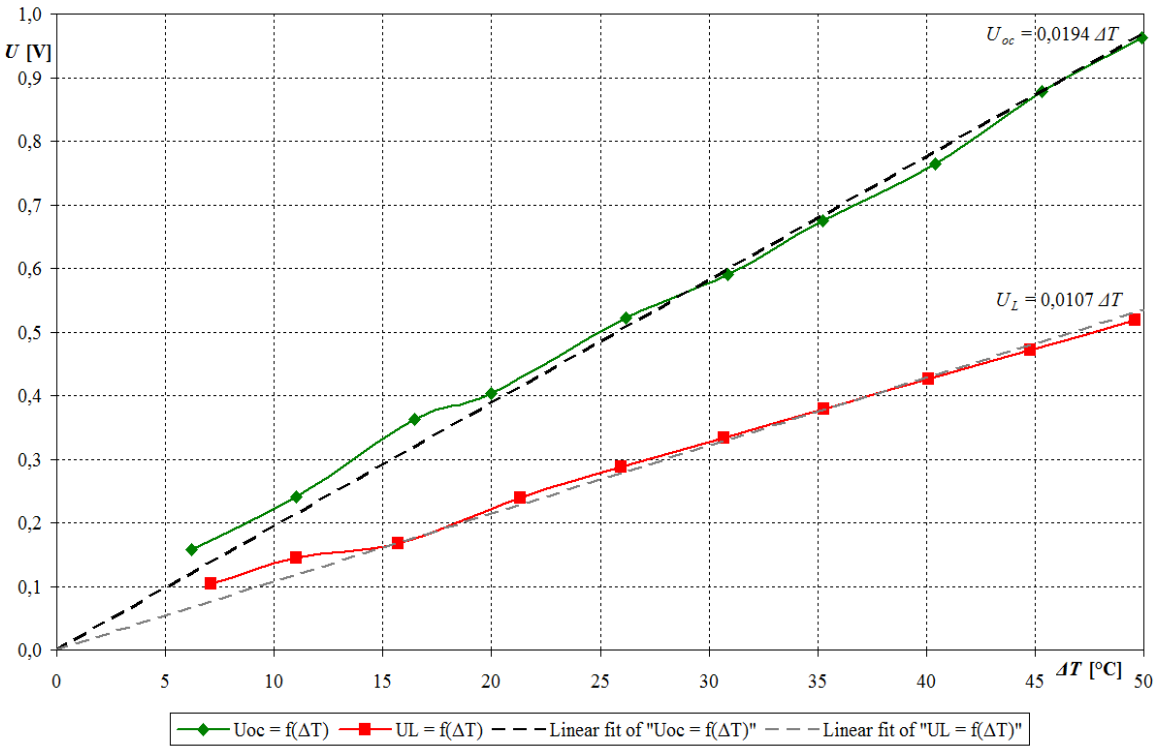

Fig. 15 – The temperature dependences of open circuit voltage U_{oc} and voltage V_L on the load R_L = 10 Ω

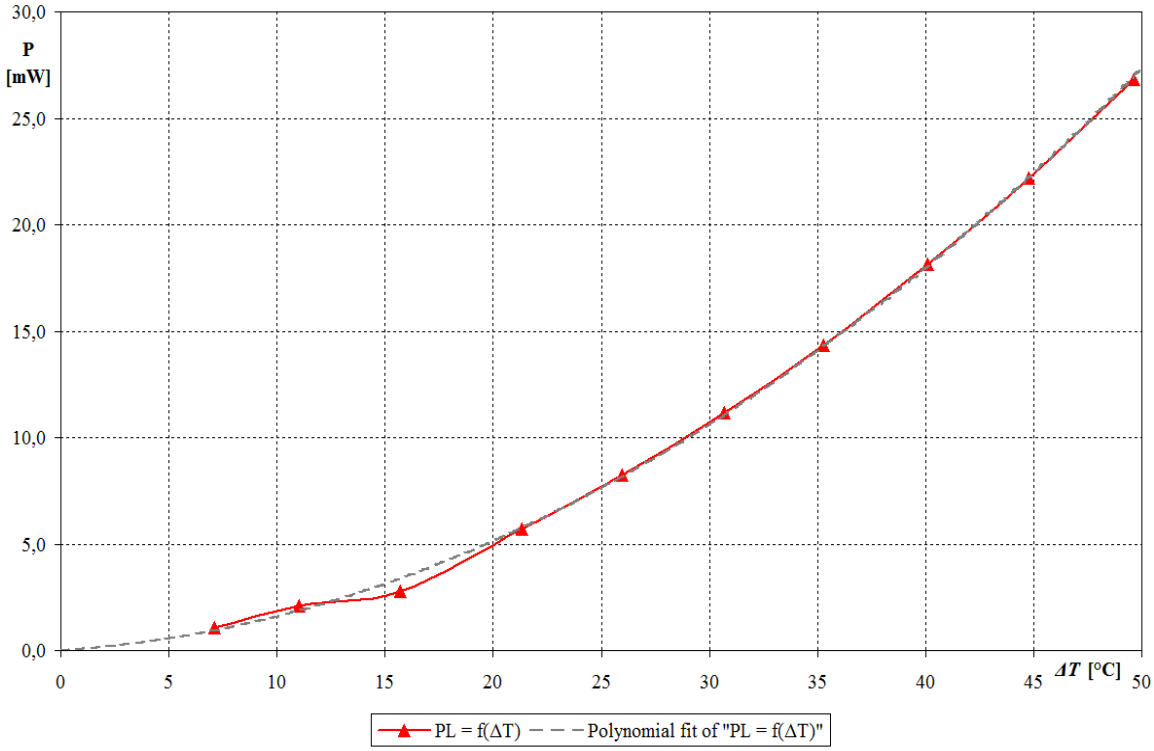

Fig. 16 – Power output when operating nearby matched load (R_L = 10 Ω)

5.4 Internal Resistance

Internal resistance of any power supply could be expressed as function of open circuit voltage, lower voltage in a loaded state and load resistance:

$$R_i = R_L\left(\frac{U_{oc}(\Delta T)}{U_L(\Delta T)} - 1\right) = R_L\left(\frac{k_{oc}}{k_L} - 1\right) \tag{5.1}$$

where:

- R_i internal resistance
- R_L load resistance
- $U_{oc}(\Delta T)$ open circuit voltage as a function of temperature difference
- $U_L(\Delta T)$ voltage on the load as a function of temperature difference
- k_{oc} slope of the open circuit voltage linear fit
- k_L slope of the linear fit of voltage on the load.

For our purposes we consider that the internal resistance is a constant in our temperature span. The data from previous measurements shown in Fig. 15 are substituted to the computation:

$$R_i = R_L\left(\frac{k_{oc}}{k_L} - 1\right) = 10.\left(\frac{0.0194}{0.0107} - 1\right) = 8.131\,\Omega \tag{5.2}$$

The internal resistance of eTEG HV56 was also measured directly using ohmmeter integrated in digital multimeter. Comparison of results is given in Tab. 5.

Tab. 5 – The internal resistance of eTEG HV56

R_i [Ω] – acquired from voltage measurement	R_i [Ω] – measured directly by ohmmeter	R_i [Ω] – extracted of datasheet characteristics
8.131	10.2 ± 0.4	10.7

Internal resistance R_i value directly measured by ohmmeter was selected as the reference for the further use. Internal resistance reached from open circuit and matched load voltage measurements is strongly influenced by measurement error. Error is given mainly by unknown values of contact resistances.

6 Modeling of MEMS TEG

There are several ways to describe a MEMS thermoelectric generator. All of the ways are based on equivalent circuit which is the simplified model of real TEG. The full equivalent circuit is mentioned in chapter 6.3. Some described modeling methods are based on further simplification of equivalent circuit.

There are no MATLAB/Simulink models of TEG in available literature. The only described Simulink model is [30] which is not a model in a true sense. The majority of existing models are implemented in SPICE [31-33].

Models described in this thesis were implemented in MATLAB/Simulink which is advantageous for the further use.

6.1 Simplified Model

The simplified model of TEG is an ideal approach for initial drafts of TEG system. Thermal part of TEG is completely removed in this case. The equation (3.1) is used for the relation between temperature difference and electrical part of TEG. Model is described in Fig. 17. [8]

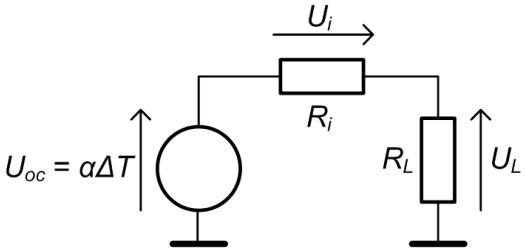

Fig. 17 – Simplified model of TEG (electrical part equivalent circuit)

Current through TEG with load is given as:

$$I = \frac{U_{oc}}{R_t} = \frac{N\alpha(T_H - T_C)}{(R_i + R_L)} \tag{6.1}$$

where:

- I current
- U_{oc} open circuit voltage
- R_t total resistance
- N number of thermocouples
- α Seebeck coefficient
- T_H temperature of the hot side
- T_C temperature of the cold side
- R_i internal resistance
- R_L load resistance.

Voltage on the load is given as:

$$U_L = U_{oc}\frac{R_L}{(R_i + R_L)} = N\alpha(T_H - T_C)\frac{R_L}{(R_i + R_L)} \tag{6.2}$$

where:

- U_L voltage on load
- U_{oc} open circuit voltage
- R_i internal resistance
- R_L load resistance.
- N number of thermocouples
- α Seebeck coefficient
- T_H temperature of the hot side
- T_C temperature of the cold side.

Power on the load is a simple product of the previous variables (6.2) and (6.1):

$$P_L = U_L I \tag{6.3}$$

where:

- P_L power on load
- U_L voltage on load
- I current.

Simulation was carried using MATLAB [App. 1]. Used input parameters are listed in Tab. 6. The results of simulation using simplified model are listed in Tab. 7.

Tab. 6 – Input parameters to simplified model

Parameter	Value
Number of thermocouples N	72
Seebeck coefficient α	382 μV/K
Temperature of the hot side T_H	{45, 85, 135} °C
Temperature of the cold side T_C	35 °C
Internal resistance R_i	10.2 Ω
Load resistance R_L	10.2 Ω (matched load)

Tab. 7 – Results from simplified model

ΔT [°C]	U_{oc} [V]	U_L [V]	I_L [mA]	P_L [mW]
10	0.275	0.138	13.482	1.854
50	1.375	0.688	67.412	46.379
100	2.750	1.375	134.824	185.383

6.2 Analytical Model of MEMS TEG with Contact Resistances

Analytical model with contact resistances is probably the most used model when dimensioning the TEG system. Model deals with realistic geometry of TEG module shown in Fig. 18. Model provides the calculation of all variables with matched load. [7, 34]

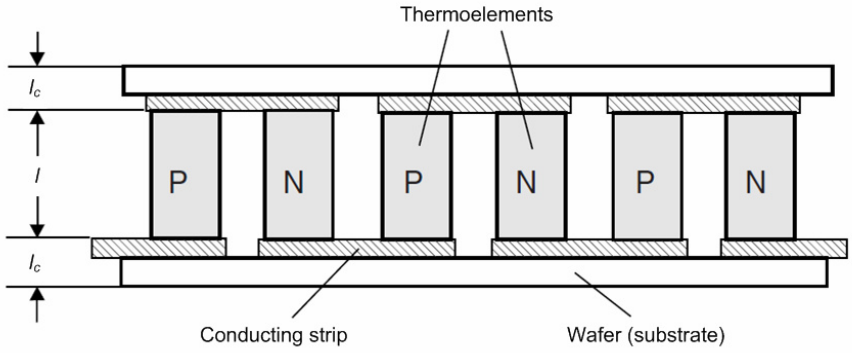

Fig. 18 – geometry of TEG model with contact resistances [7]

Voltage on matched load is given as:

$$U_L = \frac{N\alpha(T_H - T_C)}{1 + 2r\frac{l_c}{l}} \tag{6.4}$$

where:

- N number of thermocouples
- α Seebeck coefficient
- T_H temperature of the hot side
- T_C temperature of the cold side
- r thermal contact parameter
- l_c wafer thickness
- l thermoelement length.

Current through TEG with matched load is given as:

$$I = \frac{A\alpha(T_H - T_C)}{2\rho(n+l)\left(1 + 2r\frac{l_c}{l}\right)} \tag{6.5}$$

where:

- A thermocouple area
- α Seebeck coefficient
- T_H temperature of the hot side
- T_C temperature of the cold side
- ρ electrical resistivity of thermocouples material
- r thermal contact parameter
- n electrical contact parameter
- l_c wafer thickness
- l thermoelement length.

Power on the matched load is a simple product of the previous variables as usual:

$$P = \frac{\alpha_{AB}{}^2 AN(T_H - T_C)^2}{2\rho(n+l)\left(1+2r\frac{l_c}{l}\right)^2} \tag{6.6}$$

where:

- A thermocouple area
- α Seebeck coefficient
- N number of thermocouples
- T_H temperature of the hot side
- T_C temperature of the cold side
- ρ electrical resistivity of thermocouples material
- r thermal contact parameter
- n electrical contact parameter
- l_c wafer thickness
- l thermoelement length.

If needed, efficiency of TEG operating with matched load could be expressed as follows:

$$\eta = \frac{\left(\frac{T_H - T_C}{T_H}\right)}{\left(1+2r\frac{l_c}{l}\right)^2\left[2-\frac{1}{2}\left(\frac{T_H - T_C}{T_H}\right)+\left(\frac{4}{ZT_H}\right)\left(\frac{l+n}{l+2rl_c}\right)\right]} \tag{6.7}$$

where:

- T_H temperature of the hot side
- T_C temperature of the cold side
- r thermal contact parameter
- n electrical contact parameter
- l_c thermocouple length
- l wafer thickness
- ZT_H figure of merit (referenced to the hot side).

Simulation was carried using MATLAB [App. 2]. Used input parameters are listed in Tab. 8. The results of simulation using simplified model are listed in Tab. 9.

Tab. 8 – Input parameters to analytical model with contact resistances

Parameter	Value
Number of thermocouples N	72
Seebeck coefficient α	382 μV/K
Temperature of the hot side T_H	{45, 85, 135} °C
Temperature of the cold side T_C	35 °C
Thermocouple length l_c	0.07 mm
Wafer thickness l	0.25 mm
Thermoelement area A	$0.0446.10^{-6}$ m^2
Electrical resistivity of tcs material ρ	$1.6535.\ 10^{-5}$ m
Thermal contact parameter r	0.2
Electrical contact parameter n	0.1 mm
Figure of merit Z	0.75 °C^{-1}

Tab. 9 – Results from analytical model with contact resistances

ΔT [°C]	U_L [V]	I_L [mA]	P_L [mW]	η [%]
10	0.113	12.479	1.413	1.877
50	0.566	62.393	35.318	5.639
100	1.133	124.786	141.398	7.524

6.3 Equivalent Circuit

The equivalent circuit is made up of thermal and electrical part. Both parts are connected together by the Seebeck effect equation (3.1). Topology of full MEMS TEG model is given in the Fig. 19. The dashed line drawn part of equivalent circuit represents the transient behavior of MEMS TEG. The solid line drawn parts are applied in both transient- and steady-state.

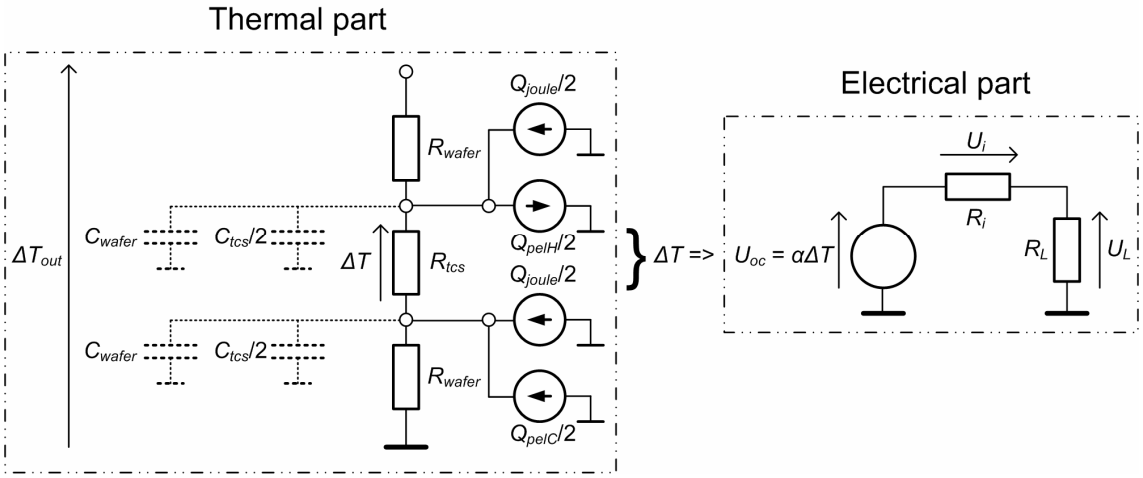

Fig. 19 – TEG equivalent circuit

The heat flux through the cold side caused by the Peltier effect is given as:

$$Q_{pelC} = NT_C I\alpha \tag{6.8}$$

where:

- Q_{pelC} heat flow through the cold side
- N number of thermocouples
- T_C temperature of the cold side
- I current
- α Seebeck coefficient.

The heat flux through the hot side caused by the Peltier effect is given as:

$$Q_{pelH} = NT_H I\alpha \tag{6.9}$$

where:

- Q_{pelH} heat flow through the hot side
- N number of thermocouples
- T_H temperature of the hot side
- I current
- α Seebeck coefficient.

Joule heating in the TEG is applied according to:

$$Q_{joule} = R_i I^2 \tag{6.10}$$

where:

- Q_{joule} Joule heating
- R_i internal resistance
- I current.

Elemental equations which describe each thermal resistances and heat masses were compiled by blocks in the Simscape toolbox of MATLAB/Simulink. Elemental equations are ensured by simply assigning of material and geometry parameters into function blocks. Used input parameters are listed in Tab. 8. The results of simulation using simplified model are listed in Tab. 9.

Both steady-state [App. 3] and dynamic [App. 4] models based on equivalent circuit were implemented. Step-response of dynamic model is shown in Fig. 20.

Tab. 10 – Input parameters to model based on equivalent circuit

Parameter	Value
Number of thermocouples N	72
Seebeck coefficient α	382 μV/K
Internal resistance R_i	10.2 Ω
Load resistance R_L	10.2 Ω (matched load)
Temperature of the hot side T_H	{45, 85, 135} °C
Temperature of the cold side T_C	35 °C
Thermocouple length l_c	0.07 mm
Wafer thickness l	0.25 mm
contact area of TEG	6.4163 mm^2
Electrical resistivity of tcs material	1.6535. 10^{-5} m
Si thermal conductivity (wafer)	130 W/(m.K)
Bi_2Te_3 thermal conductivity (tcs)	0.8815 W/(m.K)
Si specific heat (wafer)	700
Bi_2Te_3 specific heat (tcs)	160
Tcs mass	3.735 mg
Wafer mass	3.459 mg

Tab. 11 – Results from model based on equivalent circuit

ΔT_{out} [°C]	U_{oc} [V]	U_L [V]	I_L [mA]	P_L [mW]
10	0.262	0.130	12.781	1.665
50	1.312	0.651	63.784	41.552
100	2.623	1.302	127.731	166.269

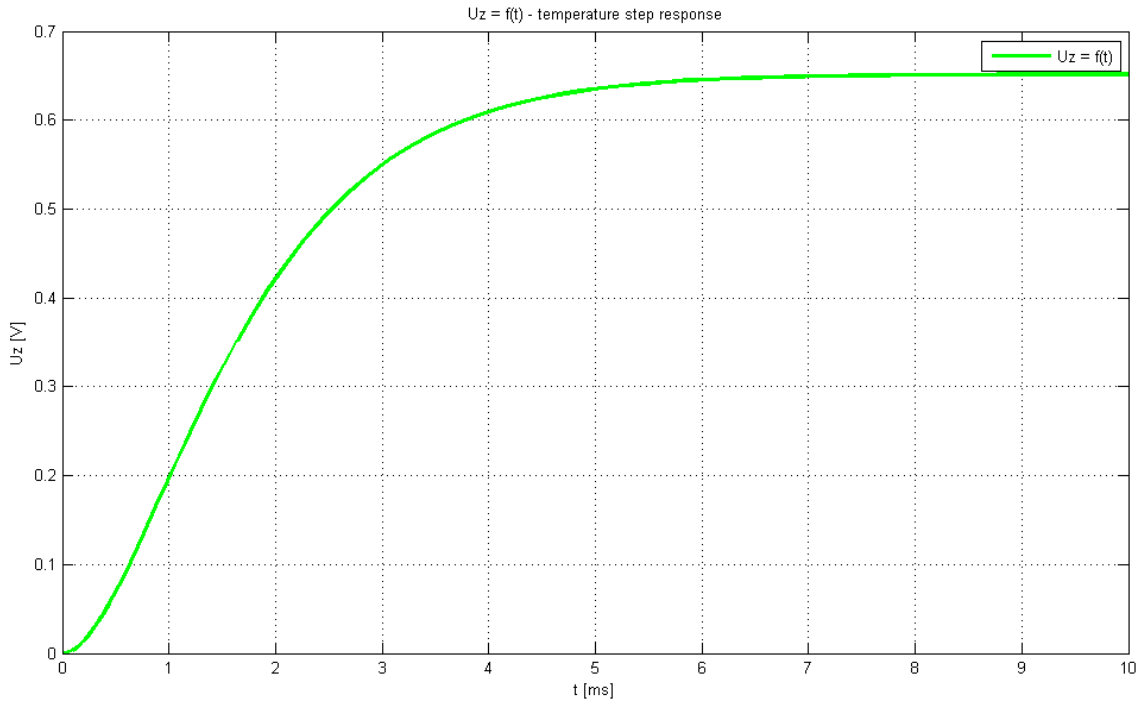

Fig. 20 – T_H step response of dynamic MEMS TEG model

7 Comparison of Results of Used Methods

All the results acquired by measurement, modeling and manufacturers datasheets are listed below. The maximal deviation between measured and datasheet value is in the case of open circuit *voltage* U_{oc} on temperature difference 50 °C – 19.8 %. The measured data exceed the model and measured data on low temperature differences. This imbalance is given by problems with maintaining the temperature on low temperature differences. The real temperature was much higher than set – for example in Tab. 4. Measured data are also loaded by error of unknown contact resistances. True temperatures on the surfaces of MEMS TEG couldn't be observed due to this problem.

All the models could be much more precise if using the input data directly given by manufacturer. For the purposes of these models were used traceable or generally known data.

Tab. 12 – Comparison of measured, datasheet and model results of eTEG HV56 – open circuit voltage

ΔT [°C]	U_{oc} [V] - measured	U_{oc} [V] - simplified model	U_{oc} [V] - Simulink model	U_{oc} [V] - analytical model	U_{oc} [V] - datasheet
10	0.241	0.275	0.262	-	0.26
50	0.962	1.375	1.312	-	1.2
100	-	2.750	2.623	-	2.5

Tab. 13 – Comparison of results – eTEG HV56 – voltage on matched load

ΔT [°C]	U_L [V] - measured	U_L [V] - simplified model	U_L [V] - Simulink model	U_L [V] - analytical model	U_L [V] - datasheet
10	0.145	0.138	0.130	0.113	0.13
50	0.518	0.688	0.651	0.566	0.6
100	-	1.375	1.302	1.133	1.25

Tab. 14 – Comparison of results – eTEG HV56 – current through matched load

ΔT [°C]	I_L [mA] - measured	I_L [mA] - simplified model	I_L [mA] - Simulink model	I_L [mA] - analytical model	I_L [mA] - datasheet
10	14.5	13.5	12.8	12.5	12
50	51.8	67.4	63.8	62.4	60
100	-	134.8	127.7	124.8	105

Tab. 15 – Comparison of results – eTEG HV56 – power on matched load

ΔT [°C]	P_L [mW] - measured	P_L [mW] - simplified model	P_L [mW] - Simulink model	P_L [mW] - analytical model	P_L [mW] - datasheet
10	2.103	1.854	1.665	1.413	1.5
50	26.830	46.379	41.552	35.318	36
100	-	185.383	166.269	141.398	130

8 TEGs in Aircraft-specific Applications

Application of TEGs as the energy harvesting systems in aerospace applications is quite a new theme which has not yet been discussed in many scientific journals apart form example [35-37]. Only functional samples of aircraft-specific TEGs were made by EADS [35].

The possible application of MEMS TEG in aircraft-specific field is their use for powering the autonomous sensor nodes (ASN) for structural health monitoring (SHM) and powering the wireless sensors in general. In comparison with other energy harvesting technologies the main advantages for the use of TEGs in aviation are no movable parts which represent low demands on maintenance. The important point is also the presence of ideal conditions for thermal energy harvesting onboard – natural heat gradient on the surface of aircraft. Other sources of heat gradient – engine, engine exhaust and heat from passengers – could be also taken into an account.

Preliminary analysis of TEGs use in aircraft showed that 0.5% or more fuel reduction is achievable. [38]

8.1 Existing Solutions

Only one experimentally tested TEG energy harvesting system for aircraft-specific field is described in [35]. The TEG is implemented into fuselage. The suitable temperature difference along the TEG is maintained using phase-change material (PCM) within whole range of aircraft operating envelope. The PCM is used for heat storage. Phase change energy is applied when the natural temperature difference along the TEG is small – during take off-and landing. System is described in the Fig. 21.

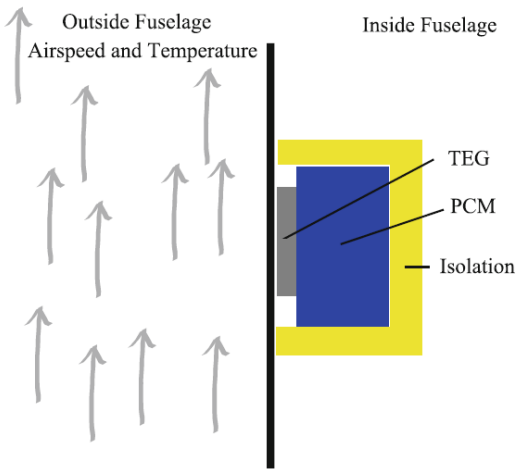

Fig. 21 – Aircraft-specific thermoelectric generator module with PCM containment [35]

8.2 Thermal Energy Harvesting Possibilities

Typical power consumption of ultra-low-power ASN is shown in the Tab. 16. TEGs are sufficient to ensure this power consumption. Power management of MEMS TEG module could be optimized using special energy harvesting electronics. Typical energy harvesting electronics is capable to operate from input sources as low as 30 mV. [39]

Tab. 16 – Typical power consumption of ultra-low-power ASN [36]

Status	Current consumption [mA]	Power consumption [mW]
Sensor sampling	0.16	0.53
Sensor switching	4.77	15.70
Sensor on	0.75	2.50
Transmission	14.95	49.30
Node idle	0.07	0.20
Average	**0.87**	**2.9**

There are many achievable technical objects with large surface temperature gradient onboard of aircraft. As an example could be served objects in the Fig. 22 and Fig. 23. – Fuel pump control unit and control unit for TJ100 turbine engine. Sharp edges of objects are evident from these pictures taken in infrared spectra. Edges between two very different colors on IR images are associated with large temperature differences. On the mentioned pictures are the temperature differences greater than 10 °C between two surrounding objects – temperature gradients. The gradients are large enough to powering the ASN mentioned above.

Temperature of TEG operation has to be in the range guaranteed by TEG manufacturer. The temperature span on the fuselage surface is given by aircraft operating envelope. Typical values are -50 °C to +50 °C. When placing TEG to some another heat gradient source the individual conditions have to be taken into account.

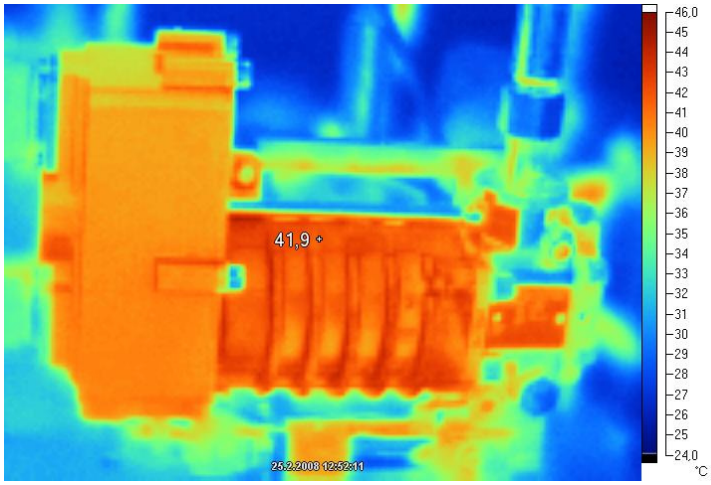

Fig.22 – Fuel pump control unit FPC [40]

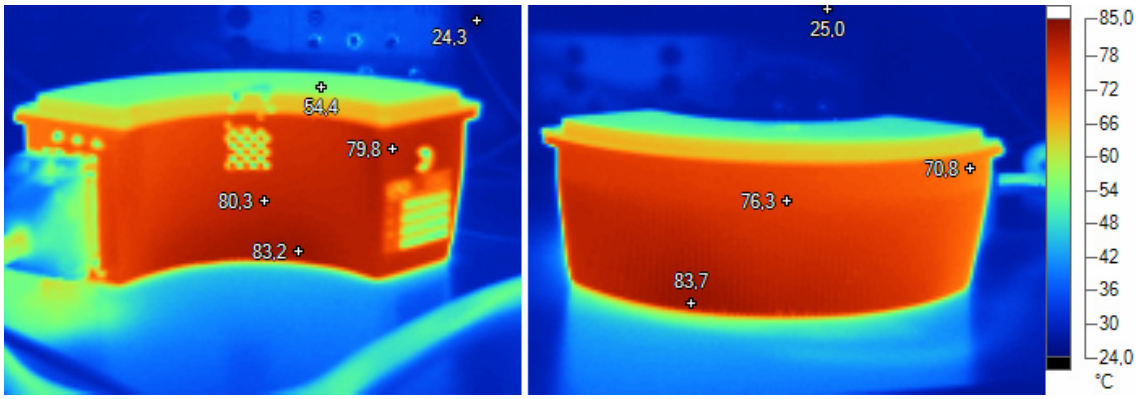

Fig. 23 – CPSJ control unit for TJ100 turbine engine [41]

Conclusion

MEMS thermoelectric generators are an area which is changing very rapidly in the laboratory environment. On the other hand, not all the things which have been developed in laboratories are turned into a practice as soon as possible. There are a few existing MEMS TEG modules on the market. These modules were described in chapter 4. Unfortunately there is a lack of reachable information about their design. Information about particular technologies used in manufacturing of commercially available MEMS TEGs was found after a long search. For the purposes of this work the Nextreme eTEG HV56 was selected.

Results of measurement on the real MEMS TEG module are listed in chapter 5. Measurement on the real MEMS TEG module was mainly the great help for broad understanding of thermoelectric generators. The basic function of module was also verified. Results of measurement are not very satisfactory due to used measurement stand originally made for classical TEG. Maximum temperature differences of 50 °C were achieved. This temperature difference is insufficient for the purposes of verification of MEMS TEG for the aircraft-specific field applications. The measurement-related problems were also the temperature ripple and inaccurate temperature regulation.

Simulations of MEMS TEG were carried out on three types of models. Simulation of MEMS TEG was a quite difficult task. The analytical model of TEG with contact resistances and model based on equivalent circuit seem to be relatively accurate models. Maximum deviation between datasheet and simulated results are up to 20 %. The simplified model of TEG is an ideal approach for initial drafts of TEG. The model based on equivalent circuit could simulate both dynamic- and steady-state of MEMS TEG. The biggest problem when building the models was an insufficient amount of input data given by manufacturer. Models would be more accurate with verified input date directly given by manufacturer.

MEMS TEG seems to be the ideal power sources for structural health monitoring and powering the autonomous sensor nodes onboard of aircraft. In chapter 8 was shown that onboard of aircraft exist suitable heat gradient sources. The only one existing solution from EADS was also described in the same chapter. The biggest problem with MEMS TEGs for use in aircraft-specific field is expected in the area of airworthiness.

There are many application-related problems with MEMS TEGs which are beyond the scope of this thesis. The topics for further discussion could be for example mounting, durability and reliability, selection of energy harvesting electronics, co-simulation with surrounding systems or airworthiness-related questions. Investigation of these problems should be the natural extension of this work and the task for a future.

References

[1] R. P. Feynman, “There’s Plenty of Room at the Bottom”, *Caltech's Engineering and Science Magazine*, Feb. 1960.

[2] Mohamed Gad-el-Hak, “The MEMS Handbook”, *CRC Press*, 2001.

[3] H.D. Espinosa and C.H. Ke, "Nanoelectromechanical Systems – Experiments and Modeling," *Applied Scanning Probe Methods, Vol. 7: Biomimetics and Industrial Applications, Springer-Verlag*, Heidelberg, 2007.

[4] Stephen D. Senturia, “Microsystem Design”, *Kluwer Academic Publishers*, 2002.

[5] Allyson L. Hartzell, Mark G. da Silva, Herbert R. Shea, “MEMS Reliability”, *Springer*, 2011.

[6] H. Julian Goldsmid, “Introduction to Thermoelectricity”, *Springer*, 2010.

[7] D.M. Rowe at al., “Thermoelectrics handbook : macro to nano / edited by D.M. Rowe.”, *Taylor & Francis Group*, 2006.

[8] Shashank Priya, Daniel J. Inman, “Energy Harvesting Technologies”, *Springer*, 2009.

[9] Wulf Glatz, Etienne Schwyter, Lukas Durrer, and Christofer Hierold, "Bi_2Te_3-Based Flexible Micro Thermoelectric Generator With Optimized Design", *Journal of Microelectromechanical Systems*, vol. 18, no. 3, June 2009.

[10] Online: http://www.micropelt.com

[11] Online: http://www.nextreme.com

[12] Marlow Industries, Inc., “TG12 – 2.5 Thermoelectric Generator (Preliminary Technical Datasheet)”, 2012.

[13] Nextreme Thermal Solutions, Inc., “eTEG HV56 datasheet”, 2012.

[14] Harald Böttner, Joachim Nurnus, Alexander Gavrikov, Gerd Kühner, Martin Jägle, Christa Künzel, Dietmar Eberhard, Gerd Plescher, Axel Schubert, and Karl-Heinz Schlereth, "New Thermoelectric Components Using Microsystem Technologies", *Journal of Microelectromechanical Systems*, vol. 13, no. 3, June 2004.

[15] Online: http://spinoff.nasa.gov/Spinoff2009/ip_4.html

[16] James J. Coleman, "Metalorganic Chemical Vapor Deposition for Optoelectronic Devices", *Proceedings of the IEEE*, vol. 85, no. 11, 1997.

[17] Online: http://www.wikipedia.org

[18] Nextreme Thermal Solutions, Inc., “Product and Technology Overview”, 2010.

[19] Dr Peter Harrop and Raghu Das, "Energy Harvesting and Storage for Electronic Devices 2010-2020", *IDTechEx Ltd*, 2010.

[20] Online: http://www.micropelt.com

[21] Online: http://www.nextreme.com

[22] Online: http://www.poweredbythermolife.com

[23] Online: http://www.hi-z.com

[24] Online: http://www.perpetuapower.com

[25] Nextreme Thermal Solutions, Inc., "eTEG HV14 datasheet", 2012.

[26] Nextreme Thermal Solutions, Inc., "eTEG HV37 datasheet", 2012.

[27] Micropelt GmbH, "MPG-D651, MPG-D751 Thin Film Thermogenerators and Sensing Devices datasheet", 2011.

[28] Micropelt GmbH, "ThermoGenerator-Package (TGP) Preliminary Datasheet", 2011.

[29] KOZÁK, J. Termoelektrický generátor. Brno: Vysoké učení technické v Brně, Fakulta strojního inženýrství, 2011. 33 s. Vedoucí bakalářské práce Ing. Radek Vlach, Ph.D.

[30] Huan-Liang Tsa and Jium-Ming Lin, "Model Building and Simulation of Thermoelectric Module Using Matlab/Simulink", *Journal of Electronic Materials*, vol. 39, no. 9, 2010.

[31] Artur Mirocha, Piotr Dziurdzia, "Improved Electrothermal Model of the Thermoelectric Generator Implemented in SPICE", *ICSES 2008 International Conference on Signals and Electrnic Systems.*

[32] Piotr Dziurdzia, Artur Mirocha, "From Constant to Temperature Dependent Parameters Based Electrothermal Models of TEG", *MIXDES 2009, 16th International Conference "Mixed Design of Integrated Circuits and Systems"*, June 25-27, 2009.

[33] Piotr Dziurdzia, "Simulation Tool for Virtual Estimation of Harvested Thermoelectric Energy Supplying Wireless Sensor Nodes", *2010 2nd International Conference on Software Technology and Engineering (ICSTE)*, 2010.

[34] D.M. Rowe, G. Min, "Design theory of thermoelectric modules for electrical power generation", *IEE Proc.-Sci. Meas. Technol.*, vol. 143, no. 6, November 1996.

[35] D. Samson, T. Otterpohl, M. Kluge, U. Schmid, Th. Becker, "Aircraft-Specific Thermoelectric Generator Module", *Journal of Electronic Materials*, vol. 39, no. 9, 2010.

[36] T. Becker, M. Kluge, J. Schalk, K. Tiplady, Ch. Paget, U. Hilleringmann, T. Otterpohl, “Autonomous Sensor Nodes for Aircraft Structural Health Monitoring”, *IEEE Sensors Journal*, vol. 9, no. 11, 2009.

[37] T. Becker, M. Kluge, J. Schalk, T. Otterpohl, U. Hilleringmann: “Power Management for Thermal Energy Harvesting in Aircrafts”, *IEEE Sensors 2008 Conference*, 2008

[38] James Huang, "Aerospace and Aircraft Thermoelectric Applications", *Boeing Research & Technology*, October, 2010

[39] T. Armstrong, "Energy Harvesting for Beginners", *Linear Technology*, 2010

[40] Zdenek Ancik, Jiri Toman, Radek Vlach, and Vladimir Hubik, "Modeling of Thermal Phenomena in Liquid Cooling System for Aircraft Electric Unit", *Industrial Electronics, IEEE Transactions on*, vol. 59, no. 9, September 2012

[41] ANČÍK, Z. Modelování tepelných procesů letecké elektroniky a problematika jejího chlazení. Brno: Vysoké učení technické v Brně, Fakulta strojního inženýrství, 2010. 51 s. Vedoucí diplomové práce Ing. Radek Vlach, Ph.D.

List of Symbols

α	Seebeck coefficient
α_A	Seebeck coefficient of material A
α_B	Seebeck coefficient of material B
A	thermocouple area
E_e	electrical energy supplied to the load
I	electrical current
I_L	electrical current through load
I_{out}	electrical current through matched load
I_{sc}	short-circuit current
k_{oc}	slope of the open circuit voltage linear fit
k_L	slope of the linear fit of voltage on the load
l	wafer thickness
l_c	thermocouple length
n	electrical contact parameter
N	number of thermocouples
η	efficiency
η_{CARNOT}	theoretical (Carnot cycle) efficiency
P_L	power on load
P_{out}	power on matched load
P_{out}/A	power density
q	heat pumped through the thermoelectric module
Q_H	heath flow through the hot side
Q_{joule}	Joule heating
Q_{max}	maximum heat flow
Q_{pelC}	heat flow through the cold side
Q_{pelH}	heat flow through the hot side
r	thermal contact parameter
R_i	internal resistance
R_L	load resistance
R_t	total resistance
R_T	thermal resistance
T	temperature
T_H	temperature of the hot side
T_C	temperature of the cold side
$T_{mean,max}$	maximum mean temperature
ΔT_{set}	set temperature difference
ΔT	temperature difference
ΔT_{max}	maximum temperature difference
ΔT_{out}	outer temperature difference
U	voltage
U_L	voltage on load
$U_L(\Delta T)$	voltage on the load as a function of temperature difference
U_{oc}	open circuit voltage
$U_{oc}(\Delta T)$	open circuit voltage as a function of temperature difference
U_{out}	voltage on matched load
ZT	figure of merit
ZT_H	figure of merit (referenced to the hot side)
π_{AB}	Peltier coefficient

λ	thermal conductivity
ρ	electrical resistivity
ASN	Autonomous Sensor Node
Bi_2Te_3	Bismuth telluride
CMOS	Complementary Metal–Oxide–Semiconductor
CVD	Chemical Vapour Deposition
EADS	European Aeronautic Defence and Space Company N.V.
FOM	figure of merit
JPL	Jet Propulsion Laboratory
MEMS	MicroElectroMechanical System
MOCVD	Metal-Organic Chemical Vapour Deposition
NEMS	NanoElectroMechanical System
PCB	Printed Circuit Board
PCM	Phase-Change Material
P-N	P-type - N-type semiconductor
PVD	Physical Vapour Deposition
SHM	Structural Health Monitoring
Si	Silicon
tcs	thermocouples
TEG	ThermoElectric Generator

Appendix

[App. 1] TEGmodel_simplified.m
[App. 2] TEGmodel_contactR.m
[App. 3] TEGmodel_steadystate.mdl
[App. 4] TEGmodel_dynamic.mdl
[App. 5] TEGmodel_parameters.m
[App. 6] eTEG_HV56_datasheet.pdf
[App. 7] Janak_Ludek_bachelor_thesis_EN.pdf